Journal of Engineering Science *Vol. XXIX, no. 3 (2022), pp. 45 - 58*
Fascicle *Electronics and Computer Science* *ISSN 2587-3474*
Topic *Microelectronics and Nanotechnologies* *eISSN 2587-3482*

https://doi.org/10.52326/jes.utm.2022.29(3).04
UDC 539.23:681.586

GAS SENSITIVE FILMS BASED ON Te-SnO_2 NANOCOMPOSITE ON FLEXIBLE SUBSTRATE

Dumitru Tsiulyanu[1], ORCID: 0000-0003-3711-4434,
Olga Mocreac[1*], ORCID: 0000-0002-4362-4556,
Andrei Afanasiev[1], ORCID: 0000-0003-1523-5542,
Eduard Monaico[2] ORCID: 0000-0003-3293-8645

[1]*CIMAN Research Centre, Department of Physics, Technical University of Moldova, 41 Dacia Blvd, MD-2060, Chisinau, Republic of Moldova*
[2]*NCMST Research Centre, Technical University of Moldova, 168 Stefan cel Mare Blvd, MD-2004, Chisinau, Republic of Moldova*
*Corresponding author: Olga Mocreac, *olga.mocreac@fiz.utm.md*

Received: 04. 27. 2022
Accepted: 06. 12. 2022

Abstract. Flexible films based on novel Te-SnO_2 nanocomposites were fabricated for detection of toxic gases at room temperature. The Te-SnO_2 nanocomposites were obtained via solvohermal recrystallization of pure crystalline tellurium in nitric acid in the presence of tin chloride. The energy-dispersive X-ray spectroscopy (EDX) and XRD analyses have shown that the Te-SnO_2 films consists of fluffy structures of tiny agglomerates of the nanodimensional irregular blocks of hexagonal Te and polycrystalline SnO_2. Both current / voltage and transient characteristics of the flexible Te-SnO_2 films were investigated at room temperature in ambiance comprising different toxic gases. The maximum selectivity was revealed toward NO_2, for which in the dynamic range of 0.5 - 5.0 ppm of NO_2, the response and recovery times are about 30 s and 150 s respectively. Analysis of the response kinetics meets the Langmuir theory of adsorption. This study revealed a simple route of fabrication of the printable Te-SnO_2 nanocomposites that can be used in electronics, inclusive for development of flexible and compostable gas sensors, operating at room temperature.

Keywords: *Nanocomposites, Te-SnO_2, Conductometric sensors, NO_2.*

Rezumat. Filme flexibile bazate pe noi nanocompozite Te-SnO_2 au fost fabricate pentru detectarea gazelor toxice la temperatura camerei. Nanocompozitele Te-SnO_2 au fost obținute prin recristalizarea solvotermală a telurului cristalin pur în acid azotic în prezență de clorură de staniu. Spectroscopia cu raze X cu dispersie energetică (EDX) și analizele XRD au arătat că filmele de Te-SnO_2 constau din structuri pufoase de aglomerate mici ale blocurilor neregulate nanodimensionale de Te hexagonal și SnO_2 policristalin. Atât caracteristicile curent/tensiune, cât și tranzitorii ale filmelor flexibile de Te-SnO_2 au fost investigate la temperatura camerei într-o ambianță cuprinzând diferite gaze toxice. Selectivitatea maximă a fost evidențiată față de NO_2, pentru care în intervalul dinamic este de 0,5 - 5,0 ppm de NO_2, timpii de răspuns și de recuperare sunt de aproximativ 30 s și, respectiv, 150 s. Analiza cineticii răspunsului

corespunde teoriei Langmuir a adsorbției. Acest studiu a dezvăluit o cale simplă de fabricare a nanocompozitelor imprimabile Te- SnO_2 care pot fi utilizate în electronică, inclusiv pentru dezvoltarea senzorilor de gaz flexibili și compostabili, care funcționează la temperatura camerei.

Cuvinte cheie: *Nanocompozite, Te-SnO_2, Senzori conductometrici, NO_2.*

1. Introduction

In the last years, printed electronics becomes very attractive due to the ability of using sustainable, compostable and recyclable materials including biobased plastics and paper in the elaboration of different flexible devices, such as photodetectors, light-emitting diodes, transistors, piezo-resistive transducers, circuit boards etc. [1-5]. Many reports are available on development of flexible gas sensors (see extensive reviews [6-7]), based on plastic, polyimide, polypyrrole or polytetrafluoroethylene and paper platforms, using active layers from two-dimensional chalcogenides $SnSe(S)_2$ [8-10], nanostructured spinel ferrite $Zn_{(x)}Fe_{(1-x)2}O_4$ [11], carbon nanotubes graphene [12-15] and others. The flexible gas sensors on paper substrates are of particular interest as they are cheap, ecological and recyclable. Besides, the paper is lighter and exhibits a lower thermal expansion coefficient (2–16 ppm/C) compared to plastic substrates (20–80 ppm/C) [16]. Were reported flexible gas sensors on paper substrates designated to detect hydrogen sulfide [17, 18] ammonia [19-21] and nitrogen dioxide [22, 23]. Hydrogen sulfide gas sensors have been fabricated via printing of polyaniline (PANI)-metal salt ($CuCl_2$) composite on a paper substrate. The resistance of the sensor drops by several orders of magnitude within exposure to H_2S and behaves irreversibly due to gas induced transformation of metal salt into resulting metal sulfide [17]. Ammonia sensors were developed using carbon nanotubes (CNT) and graphite abraded on the fibers of cellulose [19], cellulose –TiO_2 – multiwall carbon nanotube hybrid nanocomposite [20] or multilayered graphene deposited on a filter paper [21]. In all cases the effect of NH_3 consists in reversible increasing of the resistance by gas adsorption, although the sensing parameters are rather different. Thin films based on single walled carbon nanotubes and graphene were also used for the development of flexible nitrogen dioxide gas sensors [21-24]. Single walled CNTs carbon nanotube ink on a cellulosic paper was shown to detect low (~ 0.25 ppm) concentrations of nitrogen dioxide at room temperature [22]. Exposing to NO_2 vapors diminishes the resistance of the sensor. The relative change of resistance nonlinearly decreases with NO_2 concentration increase. No significant change of the baseline was observed but the recovery time is in the range of 7 min. Graphene-based, flexible NO_2 sensors on paper substrates were reported to exhibit a fast (~ 50 s) response once exposed to 200 ppm NO_2 gas, but when the supply of NO_2 is stopped the current drops by ~ 20% at 360 s and slowly decreases thereafter during a long time without reaching the initial value [24]. The overall process of fabrication of such flexible chemical sensors on paper substrates appears to be rather sophisticated. Alongside, in the last decades, the remarkable performances for the NO_2 detection have been achieved via using the thin films based on elemental tellurium and its alloys (extended reviews [25-27]). Although such films exhibit high sensitivity toward nitrogen dioxide at room temperature, their morphology, electrical properties and gas sensing properties strongly depend on fabrication technology, material composition, temperature, geometry and post fabrication treatment [28-30]. The main methods of the fabrication of gas sensitive Te based films implies the thermal vacuum evaporation of either pure polycrystalline Te or its alloys, pulsed laser deposition [31], the rf sputtering [32] or

direct vapor phase process [33] in an argon atmosphere. The films usually were grown onto hard substrates of glass Pyrex, quartz, sintered or porous alumina [34], Si / SiO_2 wafers and others.

In all cases, the growing technology of Te thin films consisted of a number of physical, chemical and electrochemical procedures, including photolithography, electrochemical pickling, thermal vacuum evaporation etc.

The present work is devoted to avoiding the mentioned above complex and costly technology of tellurium based thin films fabrication, maintaining their good gas sensitivity and room temperature operating ability. A simple technology of Te-SnO_2 nanocomposite preparation was developed via thermal dissolution of polycrystalline tellurium powder in nitric acid, followed by Te reduction in the presence of tin chloride. We also demonstrated a facile method of fabrication of thin films based on Te-SnO_2 nanocomposite paste via its painting on standard paper substrates. Being supplied with contacting electrodes these films exhibit sensitivity to toxic and dangerous chemical gasses (NO_2, H_2S, and SO_2) at concentrations of 0.5 – 10 ppm or higher. The highest sensing performance was revealed with respect to nitrogen dioxide within a dynamic range 0.5 – 5.0 ppm with fast, reversible and reproducible response time ~30 s and recovery time ~ 150 s.

2. Materials and Methods

All reagents used in the experiments were of analytical grade and used as received without further purification. HNO_3 (55%) and H_2SO_4 (57 %) were purchased from Centro – Chem but $SnCl_2$ (99.95%) from Brenntag (both Poland). The procedure of the fabrication of Te-SnO_2 nanocomposites can conventionally be divided in four steps:

1) Obtaining the tellurous acid via reaction of the pure Te powder and dilute nitric acid.
2) Obtaining of a solution of the tin chloride $SnCl_2$ via dissolving the $SnCl_2$ salt into diluted sulfuric acid.
3) Obtaining a suspension of Te and SnO_2 via mixing the solutions of tin chloride $SnCl_2$ and tellurous acid.
4) Obtaining of Te-SnO_2 paste via filtering the obtained suspension and washing the filtrate under a vacuum.

In a typical experimental procedure, the tellurium powder (purity 99.999 %) was dissolved via the hydrothermal reaction in diluted nitric acid to form the tellurous acid (H_2TeO_3) accompanied with emission of the gaseous nitric oxides (NO, NO_2).

In parallel the aqua solution of tin chloride ($SnCl_2$) has been prepared via following procedure: 1.6 g of stannous chloride was placed in a container and a solution of 4 g of H_2SO_4 diluted in 150 g of distilled water was added with continuous stirring. As a result, a transparent aqua solution of $SnCl_2$ was obtained, which further has been added to aqua solution of the tellurous acid under a strong stirring. A chemical reaction occurred that resulted in formation of a black colored suspension. The resulting solid product was collected from solution through filtering and repeatedly washing with distilled water. Finally, a viscous paste has been obtained, which then was painted by Doctor Blade coating technique onto a paper substrate forming a large flexible film (Fig.1 a), which after drying at room temperature for 24 h had a thickness of around 35 μm.

Fabricated solid films were cut using scissors for further characterization and gas sensors fabrication. The gas sensor design is schematically shown in Fig. 1b.

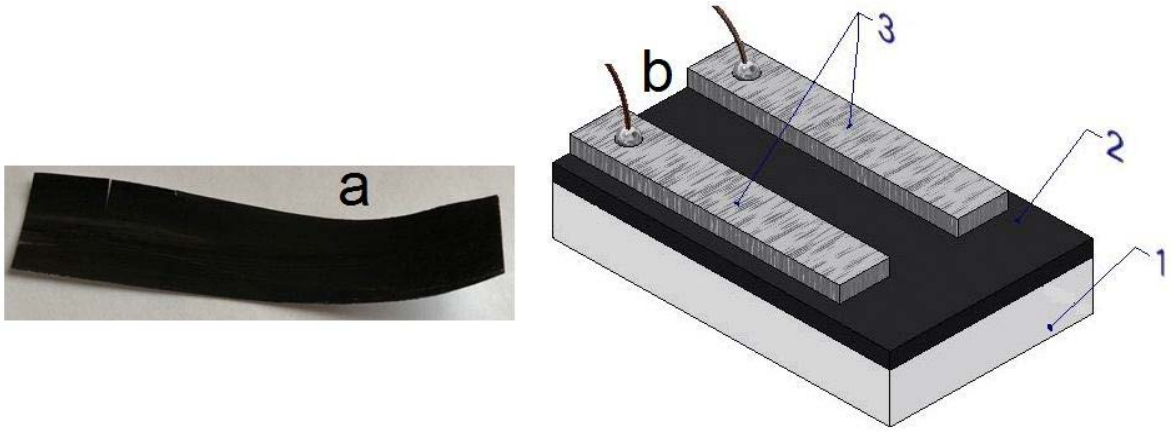

Figure 1. The view of flexible thin film based on Te-SnO_2 nanocomposite on paper substrate (a); schematic of the gas sensor design (b): 1- paper substrate; 2- active sensing Te-SnO_2 layer; 3 - metallic electrodes.

It consists of a paper substrate on which a layer of Te-SnO_2 nanocomposite is printed, above which two (or a series) of metallic (Ag, In, etc.) electrodes in a planar arrangement are deposited or painted. The sensors were encapsulated in sockets, and their contacts were thermally bonded to socket pins by means of copper wires.

Both the surface morphology and thickness of the dried films were investigated with VEGA TESCAN TS 5130 MM scanning electron microscopy (SEM). The film's elemental analysis was performed by the energy-dispersive X-ray spectroscopy (EDX) using INCA Energy 200 EDX equipment coupled with SEM. X-ray diffraction (XRD) was carried out to identify the structural phases in the grown films with a DRONE –YM1 diffractometer using Fe Kα radiations. The scattering angle was between 18 and 80 but the rotation velocity of the scintillation counter was 2 (or / and 4) angle degrees /min.

The description and detailed parameters of the gas sensing testing system, as well as of methodology of the current - voltage (I-U) and current – transient (I-t) characteristics measurement can be found in our recent publication [35]. Gaseous media with different concentration of NO_2 H_2S, NH_3, SO_2, ethanol (C_2H_5OH), acetone ($CH3)_2CO$ and toluene C_7H_8 were obtained by using the calibrated permeation or diffusion tubes (Vici Metronics, USA), which were introduced into the experimental set-up described elsewhere [36, 37].

The sensor sensitivity was defined as the relative resistance variation expressed in percent [35]:

$$S = 100\left(\left|R_a - R_g\right|\right)/R_x \quad (1)$$

where: R_a and R_g are the electrical resistances of the sensor in the air and in the presence of target gas respectively and R_x is the highest from either R_a or R_g.

The response and recovery time were estimated as the times taken to reach or to lose the 90% of steady-state values of the current respectively.

3. Results

3.1 Morphology, elemental composition and structural analysis

Figure 2 shows the typical SEM image of films fabricated in this study. The SEM reveals that Te-SnO_2 films consist of fluffy structures of tiny agglomerates of the nanodimensional irregular blocks of about 100 nm.

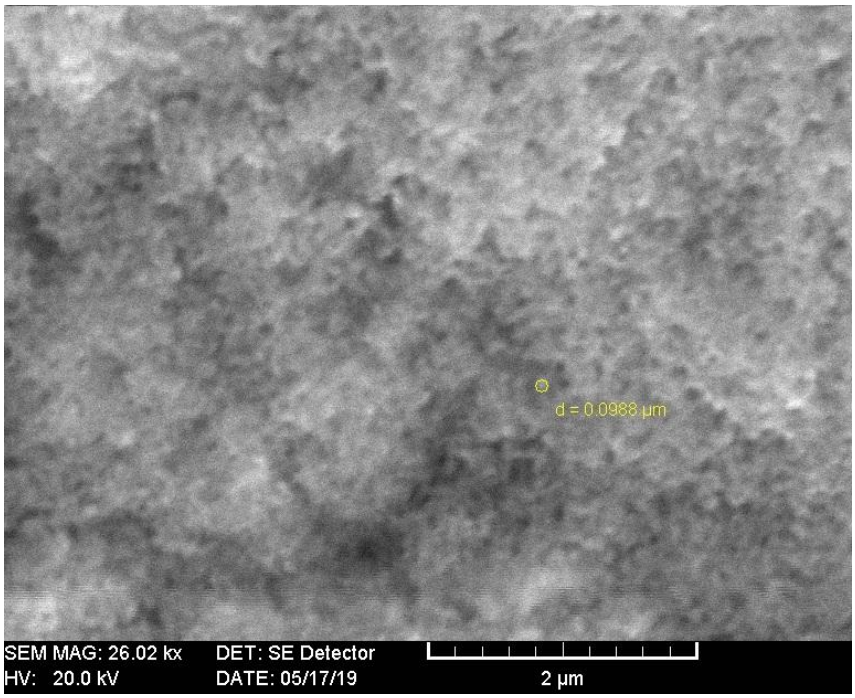

Figure 2. Typical SEM image of Te-SnO_2 based film on paper substrate.

The nanodimensional blocks were identified by energy - dispersive X-ray spectroscopy (EDX) as a composite consisting of several chemical elements. Results of EDX study of the fabricated nanocomposites are depicted in Fig. 3. As can be seen the EDX spectrum revealed the presence of about 39 at. % Te, 52 at. % O, 5.5 at. % Sn and 3.5 at % remnants of Cl.

Compositional and phase state analysis of the fabricated nanocomposite thin films have been examined by XRD, which appeared to be consistent with EDX analysis. Figure 4 displays a typical XRD pattern of the sample obtained via above-described technology along with expected location of the diffraction peaks from standard data for pure Sn [38] and TeO_2 [39] shown by colored dotted lines.

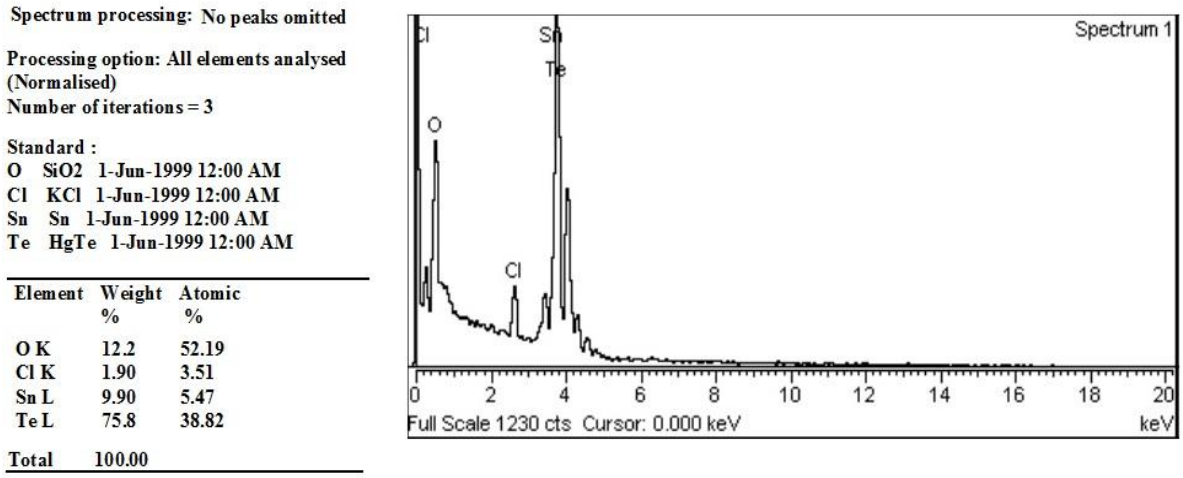

Spectrum processing: No peaks omitted

Processing option: All elements analysed (Normalised)
Number of iterations = 3

Standard :
O SiO2 1-Jun-1999 12:00 AM
Cl KCl 1-Jun-1999 12:00 AM
Sn Sn 1-Jun-1999 12:00 AM
Te HgTe 1-Jun-1999 12:00 AM

Element	Weight %	Atomic %
O K	12.2	52.19
Cl K	1.90	3.51
Sn L	9.90	5.47
Te L	75.8	38.82
Total	100.00	

Figure 3. EDX analysis of Te-SnO_2 based film.

As it is seen, all of the diffraction peaks in this pattern can be readily indexed to the hexagonal phase of tellurium with lattice constants of a = 4.46 Å and c =5.94 Å [40, 41] (JCPDS Card No.: 36-1452), along with polycrystalline tin dioxide, with predominant orientation of the crystals (110) and (002) [42, 43] (JCPDS 41-1445).

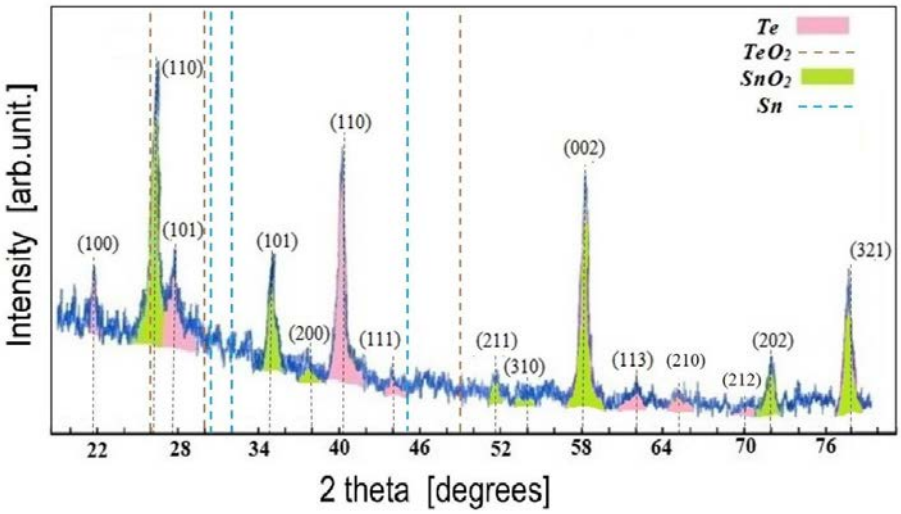

Figure 4. X-ray diffraction pattern of Te-SnO_2 nanocomposite obtained via hydrothermal reaction of tellurium powder, nitric acid and tin chloride.

3.2 Electrical conductivity at interaction with NO_2

3.2.1 Current – voltage characteristics. Effect of bending

Fig. 5 a shows the typical current /voltage characteristic of Ag/Te-SnO_2/Ag functional structures, which was measured at room temperature in ambient air and 1.0 ppm NO_2 gas, respectively. The linearly increased current, independently of the direction of the bias voltage, reflect the absence of depletion regions at the Ag contacts, i.e., they are ohmic in the entire range of applied bias voltage.

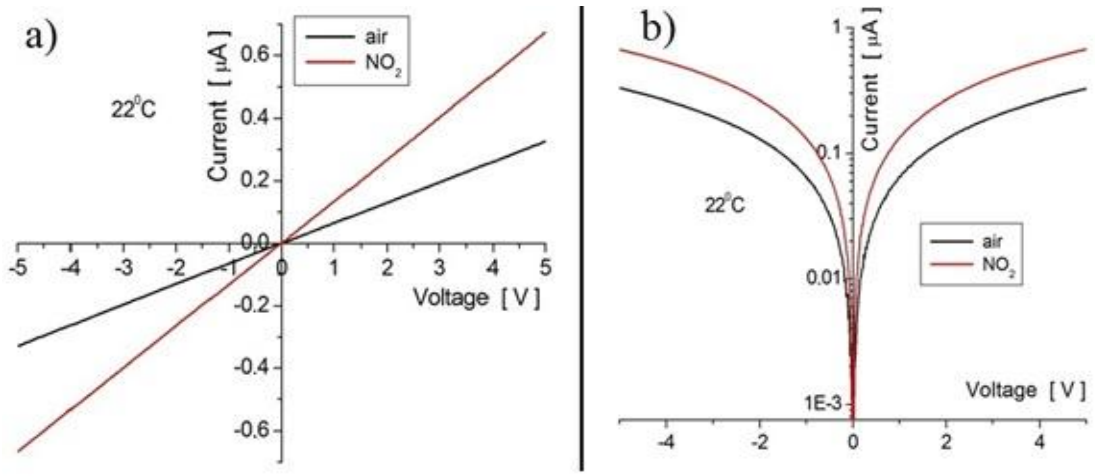

Figure 5. Current / voltage characteristic of Ag / Te-SnO_2 /Ag functional structure in air and in the presence of 1.0 ppm of NO_2 in linear (a) and semi-logarithmic scale (b).

The last is clearly confirmed by representation of I-U characteristic in a semi logarithmic scale (Fig.5 b). The influence of NO_2 gas consists in increasing of the current flow through the specimen, boosting the I-U characteristic slope. To study the effect of bending (stress) on electrical conductivity of Ag / Te-SnO_2 / Ag functional structure, its resistance has successively been measured for many times before and after bending by ~ 90 degrees. Fig. 6 shows the electrical resistance evolution of both straight and bent Ag / Te-SnO_2 / Ag functional structure grown on paper substrate in function of number of bending by ~ 90 degrees.

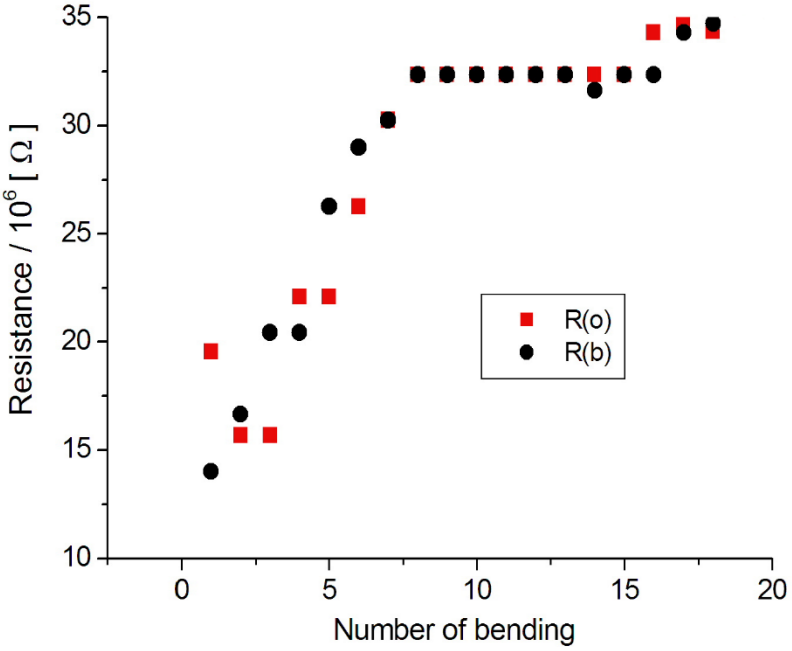

Figure 6. Evolution of electrical resistance of the straight {R(o)} and bent by 90 degrees {R(b)} Ag / Te-SnO_2 /Ag functional structure grown on paper substrate dependent of number of bending.

As can be seen, initially the resistance of both straight and bent devices increases but after approximately one dozen of bends, it tends to saturate. Moreover, for each number of bending the resistance of the straight and bended device does not differ much that confirms its flexibility.

3.2.2 Transient characteristics

Figure 7 shows the dynamic response of a Te – SnO_2 sample towards different concentrations (0.5 - 5.0 ppm) of nitrogen dioxide at room temperature and constant bias voltage, for gas pulses of similar or falling concentration (Fig 7a) as well as at increasing concentration (Fig. 7 b).

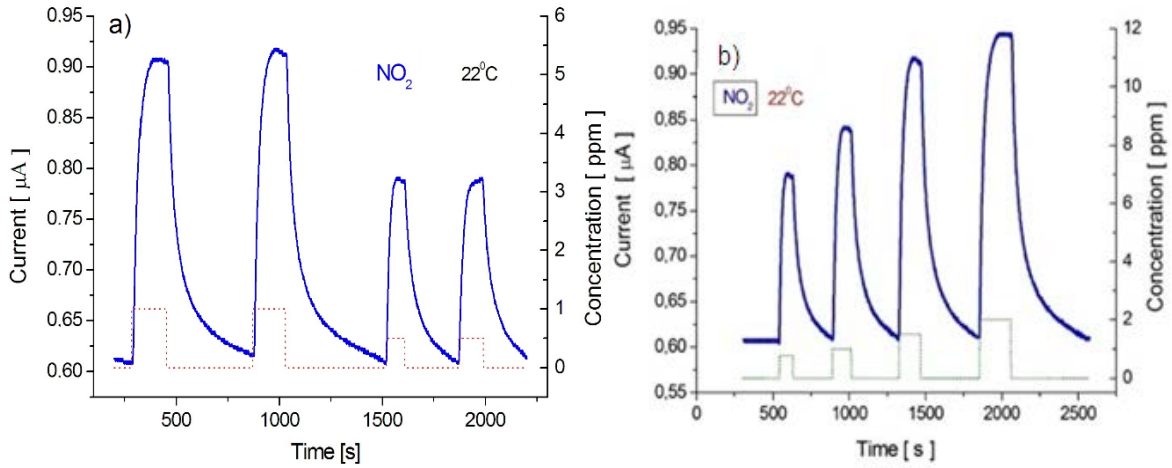

Figure 7. Transient characteristics of gas - induced current by exposure to different concentrations of NO_2 for: a) gas pulses of similar or falling concentration; b) increasing concentration. Dotted lines of the bottom show the schedule of the gas pulses.

It is seen that the sensor shows the reversible and reproducible response following the schedule of the gas application (dotted line on the bottom), without noticeable drift of the baseline. The response time is about 30 s but the recovery time is about 150 s.

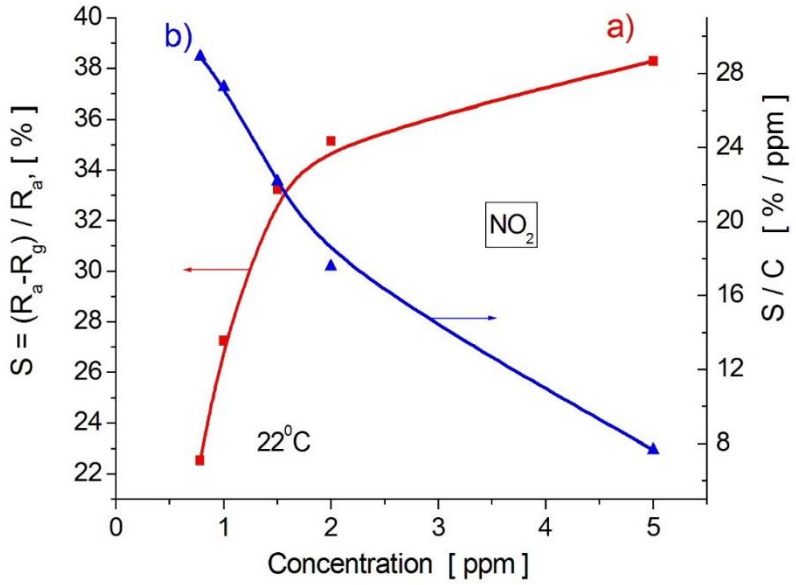

Figure 8. Sensitivity (a) and sensitivity per unit concentration (b) versus NO_2 concentration (calibration curve) at room temperature. C – is gas concentration in ppm.

Fig. 8a shows the calibration curve, that is the relative resistance variation versus gas concentrations. This curve is non-linear: the sensitivity sharply increases but tends to saturate at high NO_2 concentrations**.** As far as the sensitivity per ppm unit is concerned (Fig. 8 b), it oppositely sharply increases at low gas concentrations. Thus, the sensor is able to effectively to detect the low concentrations of NO_2, including the sub ppm range.

3.2.3 Effect of other gases and humidity

The selectivity, i.e. the effect of other gases towards Te – SnO_2 based gas sensitive device has been assessed via direct measurement of the relative variation of the resistance under exposure to H_2S, NH_3, SO_2, ethanol (C_2H_5OH), acetone $(CH_3)_2CO$ and toluene C_7H_8. It was established that ethanol, acetone, toluene and ammonia do not interact with these films as no response signal has been detected. The comparison of sensitivities to the other tested gases can be only qualitative because of very different dynamic ranges. Figure 9 shows the response of Te – SnO_2 based sensor to rectangular pulses of NO_2, H_2S and SO_2. As the ambience usually contains water vapor, we have checked the interfering effect of water vapors with NO_2 sensing at room temperature.

Fig.10 shows the sensor response toward rectangular pulses of humid air with 58% RH (shown by arrows) and 1.0 ppm NO_2 successively applied. The schedule of the NO_2 pulse application is shown by dotted line. It is seen that the effect of both H_2O and NO_2 vapors is to increase the current. Such behavior of the Te –SnO_2 based gas sensitive thin films cordially differs from behavior of the pure Te based ones, in which it was definitely pointed out that the humidification of ambiance diminishes the current flow through the sample [25]. Comparison of Figs. 7 and 10 shows that increasing RH from 20 to 58 % shifts the baseline, but the sensitivity remains nearly the same, around 30% toward 1.0 ppm NO_2.

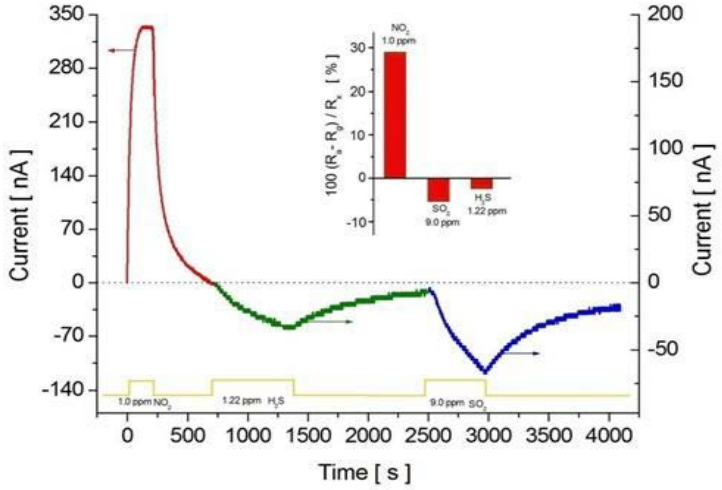

Figure 9. Transient response of a film based on Te – SnO_2 nanocomposite to rectangular pulses of NO_2, H_2S and SO_2 of different concentration and duration, shown by dotted line on the bottom. Inset shows the relative resistance change of sensor under exposure to different gases of indicated concentrations at 22 °C.

Nevertheless, it is evident that the effect of humidity is quite large and requires finding the reason, explanation and ways for its avoidance. This needs additional investigations, which are outside of the present study but are in progress.

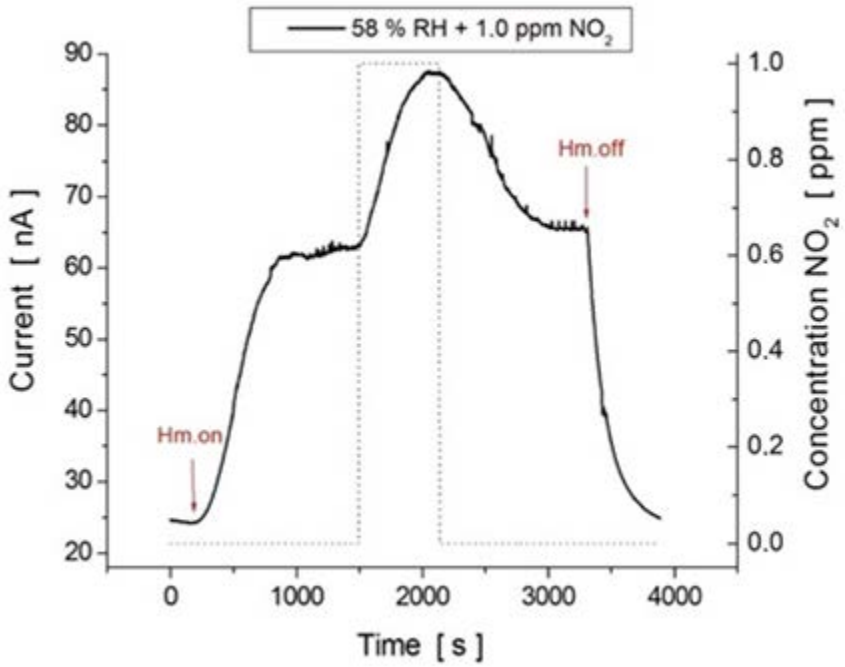

Figure 10. Effect of water vapor on the Te – SnO_2 based film by NO_2 detection at 22 °C.

4. Discussion

The chemical reactions for the synthesis of tellurium-based nanocomposites can be formulated as following: During the hydrothermal reaction, initially, tellurium powder was dissolved in dilute nitric acid to form the tellurous acid (H_2TeO_3) accompanied with emission of the gaseous nitric oxide:

$$Te + 4HNO_3 + H_2O \rightleftharpoons 3H_2TeO_3 + 4NO \quad (2)$$

Alongside, the synthesis of tellurium dioxide occurs via the reactions:

$$2Te + 9HNO_3 \rightleftharpoons Te_2O_3(OH)NO_3 + 8NO_2 + 4H_2O \quad (3)$$

$$Te_2O_3(OH)NO_3 \rightleftharpoons 2TeO_2 + HNO_3 \quad (4)$$

When the aqua solution of $SnCl_2$ has been added to the solution obtained via reactions (2-4) under a continuous stirring, the tin chloride acts as a reducing agent and the followed reaction occurs:

$$H_2TeO_3 + 2SnCl_2 \longrightarrow SnO_2 + SnCl_4 + Te \downarrow + H_2O \quad (5)$$

Thus, the resulting solid products, collected via filtering of black colored resulted suspension followed by multiple washing in distillate water, have to contain pure tellurium, tin oxide and perhaps some leftovers of $SnCl_4$. Meanwhile the XRD analysis of fabricated thin films based on synthesized via above shown reactions black solid paste (Fig.4), has confirmed the presence of hexagonal phase of tellurium alongside with polycrystalline tin dioxide but did not reveal the remainders of $SnCl_4$. Perhaps, the last is due to low amount of $SnCl_4$ in the synthesized nanocomposite that is consistent with EDX analysis. The elemental analysis of fabricated thin films performed via EDX spectroscopy (Fig.3) has identified the presence of only about 3.5 at. % remnants of Cl, alongside with about 39 at. % of the nanostructured Te.

Thus, the compositional and structural analyses of synthetized nanocomposite in conjunction with above shown experimental results related to gas sensing characterization of developed films, provides evidence that the gas sensitivity of films in question is due solely to the tellurium component that change its conductivity proportional to surface coverage [35] given by classical Langmuir's theory of adsorption [44]. The Langmuir's kinetics can be expressed in the form [45]:

$$\frac{d\theta}{dt} = \alpha C(1-\theta) - \beta\theta \quad (6)$$

where ϑ is the surface coverage that is a quantity proportional to surface concentration of adsorbed particles, C is the NO_2 concentration, α and β is the direct and inverse reaction constant respectively. According to this equation, while the surface coverage and the desorption are small, $d\theta/dt \sim (1-\theta)$. In such case, as the gas induced current in Te film is caused by releasing of majority carriers (holes) at chemical adsorption of gaseous (NO_2) species [46], the time derivative of this current, under constant bias voltage, has proportionally to decrease with ΔIincrease.

Fig. 11 shows the response current from data of Fig.7 (b) plotted, as dI/dt, a function of ΔI for several concentrations of the NO_2 applied at 22 ^{0}C. The data in this picture were averaged by 5-point smoothing. It is seen that in principle the response toward NO_2 of Te–SnO_2 based films is consistent with the Langmuir's model of surface coverage. The time derivative of the gas induced current linearly diminishes with change current increase, at that these derivative increases with gas concentration increase and even the slope change of line $dI/dt = f(C)$can be observed.

Finally, it is worth noting that the SnO_2 nanoparticles of nanocomposite in question were not observed to participate in the gas sensing process, that obviously is caused by sensor low operation temperature (~ 22 ˚C). Tin oxide becomes gas (NO_2) sensitive only at operation temperature higher than 200 ˚C [47, 48]. At that, SnO_2 does not disturb the gas sensing properties of Te nanoparticles from nanocomposite but can be the reason for large influence of the humidity.

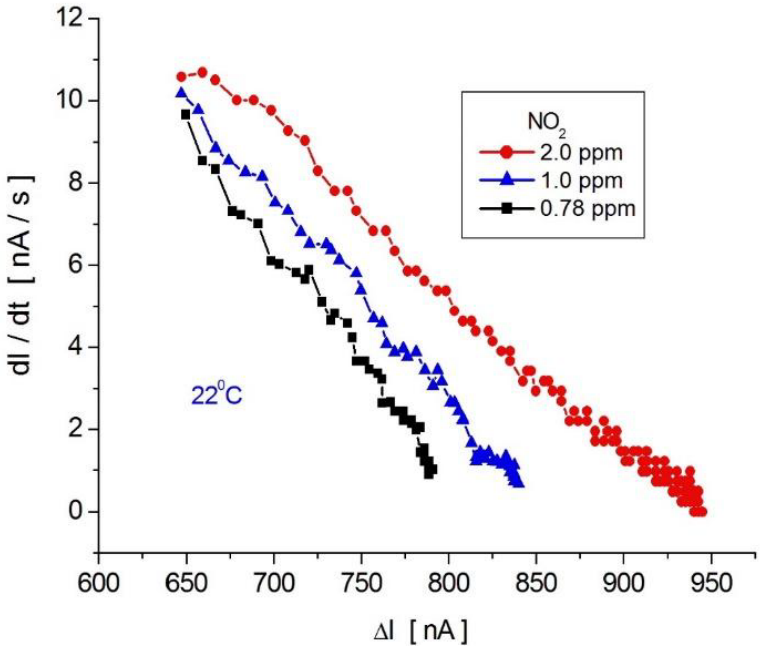

Figure 11. The Langmuir plot of the sensor response toward a rectangular pulse of NO_2 drawn using the data shown in Fig.6 for the Ag / Te - SnO_2 / Ag device.

5. Conclusions

Nano-composites of Te-SnO_2 were synthesized via a simple thermal dissolution of polycrystalline tellurium powder in nitric acid, followed by its chemical reduction in the presence of tin chloride solution. Showed by SEM, EDX and XRD analyses the composites consists of nanoparticles of around 100 nanometers, comprising about 40 at. % Te and 6.0 at. % of tin oxide. The synthesized nanocomposites can be used for fabrication of thin flexible gas sensors via screen printing technology, onto paper sheets. Such sensors exhibit selective and rapid (~30 s) response to nitrogen dioxide and operate at room temperature.

Acknowledgments. This work was supported by National Agency for Research and Development of Moldova, project PS 20.80009.5007.21. Author expresses his gratitude to Dr. G. F. Volodina at Institute of Applied Physics of MER RM for XRD analysis.

Conflicts of Interest. The authors declare no conflict of interest.

References

1. Siegel, A. C.; Phillips, S.T.; Dickey, M. D.; Lu, N.; Suo, Z.; Whitesides, G. M. Foldable Printed Circuit Boards on Paper Substrates. *Advanced Functional Materials* 2010, 20, 28–35., https://doi.org/ 10.1002/ adfm.200901363.
2. Kurra, N.; Dutta, D.; Kulkarni, G.U. Field Effect Transistors and RC Filters from Pencil-Trace on Paper. *Physical Chemistry Chemical Physics* 2013; 15 , 8367–8372., https://doi.org/10.1039/C3CP50675D.
3. Zhang, Y.; Ge, L.; Li, M.; Yan, M.; Yu, J.; Song, X.; Cao, B. Flexible Paper-Based ZnO Nanorod Light-Emitting Diodes Induced Multiplexed Photoelectrochemical Immunoassay. *Chem. Commun* 2014; 50, 1417–1419. https://doi.org/10.1039/C3CC48421A.
4. Zheng, Z.; Zhang, T.; Yao, J.; Zhang, Y.; Xu, J.; Yang, G. Flexible, Transparent and Ultra-Broadband Photodetector Based on Large-Area WSe_2 Film for Wearable Devices. *Nanotechnology* 2016; 27, 225501. https://doi.org/10.1088/0957-4484/27/22/225501
5. Tannarana, M.; Solanki, G. K.; Bhakhar, S. A.; Patel, K. D.; Pathak, V. M.; Pataniya, P. M. 2D-$SnSe_2$ Nanosheet Functionalized Piezo-resistive Flexible Sensor for Pressure and Human Breath Monitoring. *ACS Sustainable Chem. Eng.* 2020, 8, 7741−7749. https://doi.org/10.1021/acssuschemeng.0c01827.
6. Alrammouz, R.; Podlecki, J.; Abboud, P.; Sorli, B.; Habchi, R. A review on flexible gas sensors: From materials to devices. *Sensors and Actuators A* 2018; 284, 209-231. https://doi.org/10.1016/j.sna.2018.10.036.

7. Wang, T.; Guo, Y.; Wan, P.; Zhang, H.; Chen, X.; Sun, X. Flexible Transparent Electronic Gas Sensors, *Small-Wiley Online Library* 2016, 12, 28, 3748-3756. https://doi.org/10.1002/smll.201601049.
8. Chen, M.; Li, Z.; Li, W.; Shan, C.; Li, W.; Li, K.; Gu, G.; Feng, Y.; Zhong, G.; Wei, L.; Yang, C. Large-Scale Synthesis of Single-Crystalline Self-Standing $SnSe_2$ Nanoplate Arrays for Wearable Gas Sensors. *Nanotechnology* 2018; 29, 455501. https://doi.org// 10.1088/1361-6528/aade32.
9. Pawar, M.; Kadam, S.; Late, D. J. High-Performance Sensing Behavior Using Electronic Ink of 2D $SnSe_2$ Nanosheets. *Chemistry Select* 2017, 2, 4068–4075. https://doi.org/10.1002/slct.201700261.
10. Pyeon, J. J.; Baek, I-H.; Song, Y. G.; Kim, G. S.; Cho, A-J.; Lee, G-Y.; Han, J. H.; Chung, T-M.; Hwang, C. S.; Kang, C-Y.; Kim, S. K. Highly sensitive flexible NO_2 sensor composed of vertically aligned 2D SnS_2 operating at room temperature. *Journal of Materials Chemistry C* 2020, 34. https://doi.org/10.1039/D0TC02242J
11. Goutham, S.; Sadasivuni, K. K.; Kumarc, D. S.; Rao, K.V. Flexible ultra-sensitive and resistive NO_2 gas sensor based on nanostructured $Zn(x)Fe(1-x)2O_4$, RSC Adv. 2018, 8, 3243–3249. https://doi.org/10.1039/c7ra10478b.
12. Bohao, L.; Liu, X.; Yuan, Z.; Tai, H. A flexible NO_2 gas sensor based on polypyrrole/nitrogen-doped multiwall carbon nanotube operating at room temperature. *Sensors and Actuators B* 2019, 295, 86-92, https://doi.org/10.1016/j.snb.2019.05.065
13. Agarwal, P. B.; Alam, B.; Sharma, D. S.; Sharma, S.; Agarwal, A. Flexible NO_2 gas sensor based on single-walled carbon nanotubes on polytetrafluoroethylene substrates. *Flexible and Printed Electronics* 2018, 3, 035001. https://doi.org/10.1088/2058-8585/aacc8f.
14. Jeong, H. Y.; Lee, D-S.; Choi, H. K.; Lee, D. H.; Kim, J-E.; Lee, J. Y.; Lee, W. J.; Kim, S. O.; Choi, S.-Y. Flexible room-temperature NO_2 gas sensors based on carbon nanotubes/reduced grapheme hybrid films. *Applied Physics Letters* 2010, 96, 213105. https://doi.org/10.1063/1.3432446.
15. Lee, C.; Ahn, J.; Lee, K. B.; Kim, D.; Kim, J. Graphene-based flexible NO_2 chemical sensors. *Thin Solid Films* 2012, 520, 5459-5462. https://doi.org/10.1016/j.tsf.2012.03.095.
16. Alrammouza, R.; Podlecki, J.; Abboud, P.; Sorli, B.; Habchi, R. A review on flexible gas sensors: From materials to devices. *Sensors and Actuators A,* 2018, 284, 209–231. https://doi.org/10.1016/j.sna.2018.10.036
17. Sarfraz, J.; Maattanen, A.; Ihalainen, P.; Keppeler, M.; Linden, M.; Peltonen, J. Printed copper acetate based H_2S sensor on paper substrate. *Sensors and Actuators* B 2012, 173, 868–873. http://dx.doi.org/10.1016/j.snb.2012.08.008
18. Sarfraz, J.; Ihalainen, P.; Määttänen, A.; Peltonen, J.; Lindén, M. Printed hydrogen sulfide gas sensor on paper substrate based on polyaniline composite. *Thin Solid Films* 2013, 534, 621–628. http://dx.doi.org/10.1016/j.tsf.2013.02.055
19. Mirica, K. A.; Weis, J. G.; Schnorr, J. M.; Esser, B.; Swager ,T. M. *Mechanical Drawing of Gas Sensors on Paper*. Angewandte Chemie Int. Edition 2012, 51, 10740–10745. https://doi.org/10.1002/anie.201206069
20. Mun, S.; Chen, Y.; Kim, J.; Cellulose–titanium dioxide–multiwalled carbon nanotube hybrid nanocomposite and its ammonia gas sensing properties at room temperature. *Sensors and Actuators B* 2012, 171– 172, 1186– 1191, http://dx.doi.org/10.1016/j.snb.2012.06.066
21. Ghosh, R.; Singh, A.; Santra, S.; Ray, S. K.; Chandra, A.; Guha, P. K. Highly sensitive large-area multi-layered graphene-based flexible ammonia sensor. *Sensors and Actuators B* 2014, 205, 67–73. http://dx.doi.org/10.1016/j.snb.2014.08.044
22. Ammu, S.; Dua, V.; Agnihotra, S. R.; Surwade, S. P.; Phulgirkar, A.; Patel, S.; Manohar, S. K. Flexible, All-Organic Chemiresistor for Detecting Chemically Aggressive Vapors. *Journal of the American Chemical Society* 2012, 134, 4553–4556. http://dx.doi.org/10.1021/ja300420t |
23. Hassinen, J.; Kauppila, J.; Leiro,J.; Määttänen, A.; Ihalainen, P.; Peltonen, J.; Lukkari, J. Low-cost reduced graphene oxide-based conductometric nitrogen dioxide-sensitive sensor on paper. *Analytical and Bioanalytical Chemistry* 2013, 405, 3611-3617. http://dx.doi.org/10.1007/s00216-013-6805-5.
24. Yang, G.; Lee, C.; Kim, J.; Renb, F.; Pearton, S. J. Flexible graphene-based chemical sensors on paper substrates. *Physical Chemistry Chemical Physics* 2013, 15, 1798. http://dx.doi.org/: 10.1039/c2cp43717a.
25. Tsiulyanu, D. Tellurium thin films in sensor technology. Nanotechnological Basis for Advanced Sensors, Springer 2011, 363-380.
26. Petcov, P.; Tsiulyanu, D.; Kulisch, W.; Popov, C. *Nanoscience Advances in CBRN Agents Detection, Information and Energy Security: An Intoduction*. Springer 2015, 3-13. ISBN: 978-94-017-9697-2
27. He, Z.; Yang, Y.; Liu, J-W.; Yu, S-H. Emerging tellurium nanostructures: controllable synthesis and their applications. *Chemical Society Reviews* 2017, 46, 2732—2753. https://doi.org/10.1039/c7cs00013h.

28. Tsiulyanu, D.; Marian, S.; Miron, V.; Liess, H - D. High sensitive tellurium based NO_2 gas sensor. *Sensors and Actuators B* 2001, 73, 35 – 39. https://doi.org/10.1016/s0925-4005(00)00659-6.
29. Tsiulyanu, D.; Tsiulyanu, A.; Liess, H-D.; Eisele, I. Characterization of tellurium-based films for NO_2 detection. *Thin Solid Films* 2005, 485, 252 -256. https://doi.org/10.1016/j.tsf.2005.03.045.
30. Wüsten, J.; Potje-Kamloth, K. Chalcogenides for thin film NO sensors. *Sensors and Actuators B* 2010, 145, 216–224. https://doi.org/10.1016/j.snb.2009.11.058
31. Popescu, M.; Velea, A.; Sava, F.; Lorinczi, A.; Tomescu, A.; Simion, C.; Matei, E.; Soco, G.; Mihailescu, I. N.; Andonie, A.; Stamatin, I. Structure and properties of silver doped $SnSe_2$ and $Ge_2Sb_2Te_5$ thin films prepared by pulsed laser deposition. *Physica Status Solidi A* 2010, 207, 516–520. https://doi.org/10.1002/pssa.200982900
32. Siciliano, T.; Giulio, M. Di.; Tepore, M.; Filippo, E.; Micocci, G.; Tepore, A. Tellurium sputtered thin films as NO_2 gas sensors. *Sensors and Actuators B* 2008, 135, 250-256. https://doi.org/10.1016/j.snb.2008.08.018.
33. Her, Y.C.; Huang, S.L. Growth mechanism of Te nanotubes by a direct vapor phase process and their room temperature CO and NO_2 sensing properties. *Nanotechnology* 2013, 24, 215603, 9. https://doi.org/10.1088/0957-4484/24/21/215603.
34. Tsiulyanu, D. Gas-sensing features of nanostructured tellurium thin films. *Beilstein J. Nanotechnology* 2020, 11, 1010–1018. https://doi.org/10.3762/bjnano.11.85.
35. Tsiulyanu, D. Conductometric NO_2 gas sensor based on nanolayered amorphous tellurium for room temperature operation. *Sensors and Actuators B* 2022, 352, https://doi.org/10.1016/j.snb.2021.131034
36. Cabala, R.; Meister, V.; Potje-Kamloth, K.; Effect of competitive doping on sensing properties of polypyrrole. *Journal of the Chemical Society, Faraday Transactions* 1997, 9, 131-137. https://doi.org/10.1039/A604780G
37. Tsiulyanu, D.; Ciobanu, M. Impact of adsorbed gases on the transport mechanisms in $Ge_8As_2Te_{13}S_3$ amorphous films. *Glass Physics and Chemistry* 2019, 45, 53–59. https://doi.org/10.1134/S1087659619010140.
38. Hu, R.; Sun, W.; Zeng, M.; Zhu, M. Dispersing SnO_2 nanocrystals in amorphous carbon as a cyclic durable anode material for lithium-ion batteries. *Journal of Energy Chemistry* 2014, 23, 338–345. https://doi.org/10.1016/S2095-4956(14)60156-X.
39. Shen, Y.; Fan, A.; Wei, D.; Gao, S.; Liu, W.; Hana, C.; Cuia, B. A low-temperature n-propanol gas sensor based on TeO_2 nanowires as the sensing layer. *RSC Advances* 2015, 5, 29126–29130. https:// doi.org/10.1039/C5RA00867K.
40. Liang, F.; Qian, H. Synthesis of tellurium nanowires and their transport property. M*aterials Chemistry and Physics* 2009, 113, 523–26.
41. Wang, S.; Wen, H.; Guan, W.; Zhang, L.; Zhang, D.; Huang, S.; Wang, J. Fabricating two-dimensional nanostructured tellurium thin films via pyrolyzing a single-source molecular precursor. *Thin Solid Films* 2010, 518, 4215–20. https://doi.org/10.1016/j.tsf.2009.12.081
42. Bhagwat, A. D.; Sawant, S. S.; Ankamwar, B. G.; Mahajan, C. M. Synthesis of Nanostructured Tin Oxide (SnO_2) Powders and Thin Films Prepared by Sol-Gel Method. *Journal of Nano-and Electronic Physics* 2015, 7, 4, 04037.
43. Li, I.; Chen, C.; Li, J.; Li, S.; Dong, C. Synthesis of tin-glycerate and its conversion into SnO_2 spheres for highly sensitive low-ppm-level acetone detection. *Journal of Materials Science: Materials in Electronics* 2020, 31, 16539–16547. https://doi.org/10.1007/s10854-020-04208-7.
44. Volkenstein, T. *Electronic Processes on Semiconductor Surfaces During Chemosorption.* A Division of Plenum Publishing Corporation, Consultants Bureau, New York, 1987, 427pp.
45. Filippini, D.; Rosch, M.; Aragon, R.; Weimar, U. Field-effect NO_2 sensors with group 1B metal gates. *Sensors Actuators B* 2001, 81, 83–87. https://doi.org/10.1016/S0925-4005(01)00935-2.
46. Tsiulyanu, D.; Ciobanu, M.; Mocreac, O. *Impedance Characterization of Gas Sensitive Chalcogenide Films*. Springer 2017, 317-332, https://doi.org/10.1007/978-94-024-1298-7_31.
47. Gopel, W.; Schierbaum, K.-D.; SnO_2 sensors: current status and future prospects. *Sensors and Actuators B* 1995, 26–27, 1–12. https://doi.org/10.1016/0925-4005(94)01546-T
48. Shi, L.; Hasegawa, Y.; Katsube, T.; Onoue, K.; Nakamura, K.; Highly sensitive NO_2 gas sensor fabricated with RF induction plasma deposition method. *Sensors and Actuators B* 2004, 99, 361-366. https://doi.org/10.1016/j.snb.2003.12.003.

Citation: Tsiulyanu, D.; Mocreac, O.; Afanasiev, A.; Monaico, E. Gas sensitive films based on Te-SnO_2 nanocomposite on flexible substrate. *Journal of Engineering Science* 2022, 29 (3), pp. 45-58. https://doi.org/10.52326/jes.utm.2022.29(3).04.

Submission of manuscripts: jes@meridian.utm.md